

Supplementary Information

Revisiting Stress-Strain Behavior and Mechanical Reinforcement of Polymer Nanocomposites from Molecular Dynamics Simulations

Jianxiang Shen, ^{*a,b} Xiangsong Lin, ^{a,b} Jun Liu, ^c and Xue Li^{*a,b}

^a Key Laboratory of Yarn Materials Forming and Composite Processing Technology of Zhejiang Province, Jiaxing
314001, P.R. China

^b Department of Polymer Materials and Engineering, Jiaxing University, Jiaxing 314001, P.R. China

^c Beijing Engineering Research Center of Advanced Elastomers, Beijing University of Chemical Technology,
Beijing 100029, P.R. China.

Corresponding author

*Email: shenjx@zjxu.edu.cn (J. Shen); lixue_zjxu@163.com (X. Li)

Number of Pages: 15

Number of Figures: 5

Number of Tables: 4

CONTENTS

Part I. Estimation Methods of Percolation Threshold

Part II. Comparison of Simulation Results with Experimental Data

- (1) Comparison of the Payne effect of Polymer Nanocomposites
- (2) Comparison of the Mechanical Reinforcement of Polymer Nanocomposites
- (3) Comparison of Activation Energy of Polymer Nanocomposites

Fig. S1. Comparison of stress-strain curves at the tensile rates of (a)(c) $0.0327/\tau$ and (b)(d) $0.00327/\tau$.

Fig. S2. (a) Snapshot of equilibrated simulation systems at the volume fraction of 9.30% and 17.01%. (b) Young's modulus as a function of volume fraction. The nanoparticle diameter is $D=4$, and the particle-polymer interaction strength is $\varepsilon_{np}=1.0$. (c) Probability of network formation as a function of nanoparticle volume fraction for different simulated systems. (d) Comparison of the percolation threshold ϕ_{cm} from the mechanical reinforcement method and that from nanoparticle cluster percolation analysis ϕ_{cn}

Fig. S3. Mechanical reinforcement extent, in terms of Young's modulus of nanoparticle-filled systems normalized by that of unfilled system, as a function of filler volume fraction. References are listed below. Details of filler parameters are shown in Table S3.

Fig. S4. The bond orientation $\langle P_2 \rangle$ as a function of strain at different system temperatures. ($D=4$, $\phi=17.01\%$, $\varepsilon_{np}=1.0$ and $\varepsilon_{nn}=1.0$)

Fig. S5. Stress-strain curves with different nanoparticle diameters at a volume fraction of $\phi=17.01\%$.

Table S1. Comparison of the Payne effect extracted from the current MD simulation study and the literatures relating to experiment research

Table S2. Polymer Abbreviations

Table S3. Some Filler Parameters in the literatures relating to experiment research

Table S4. Activation energy derived from experiment research

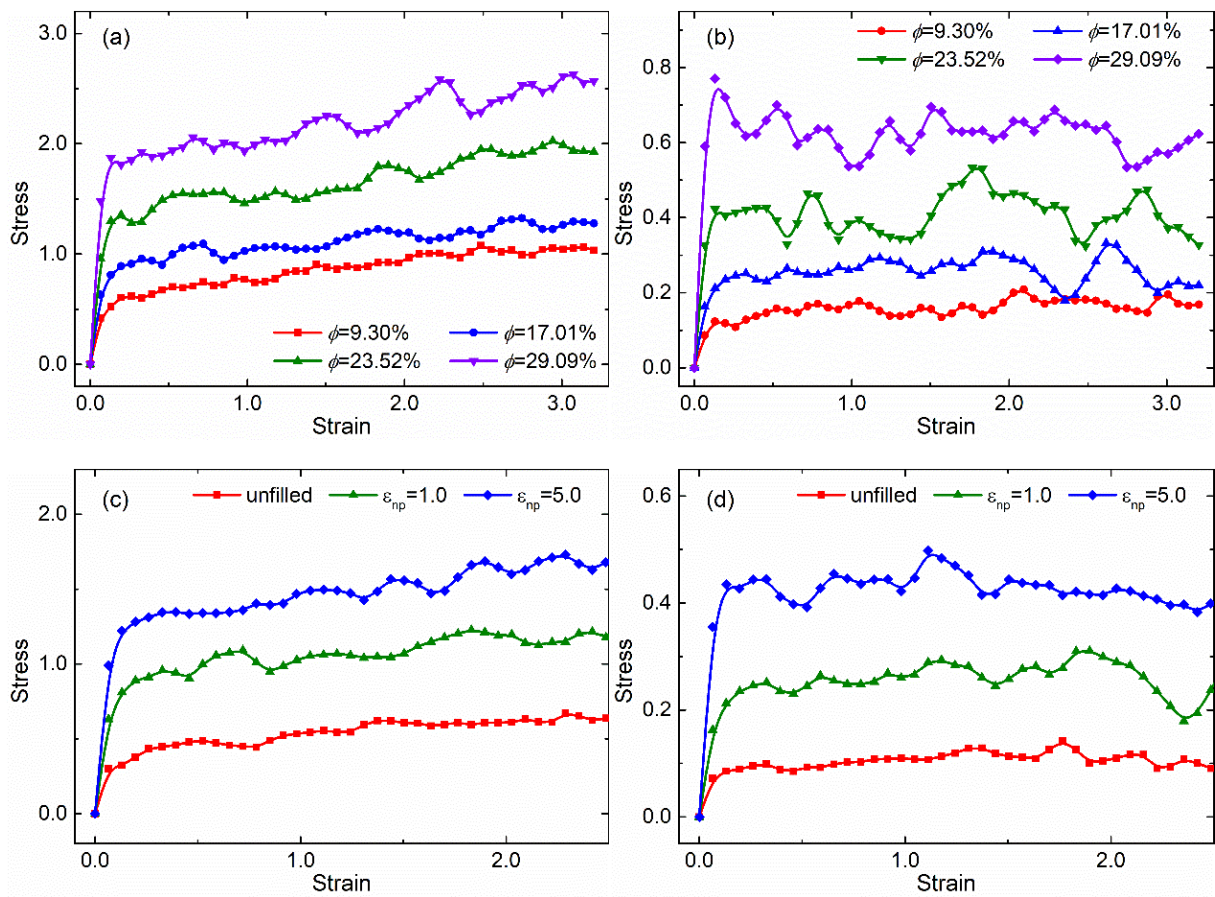


Fig. S1. Comparison of stress-strain curves at the tensile rates of (a)(c) $0.0327/\tau$ and (b)(d) $0.00327/\tau$

Part I. Estimation Methods of Percolation Threshold

From the snapshots below showing the spatial distribution of nanoparticles ($D=4\sigma$), it can be inferred that the percolation transition would occur at a volume fraction between 9.30% and 17.01%. One common method for estimating the percolation threshold is to find the intersection point of the two fitted lines of mechanical reinforcement (e.g., Young's modulus) far below and far above the percolation threshold [1-2], as indicated by Fig. S2 below. From Fig. S2, it is seen that the percolation threshold (ϕ_{cm}) is approximately 15% ($\pm 2\%$), which is within the range for rigid fillers in soft polymers, i.e., 6-35% depending on the nanoparticle size and shape, and particle-polymer interaction strength [3].

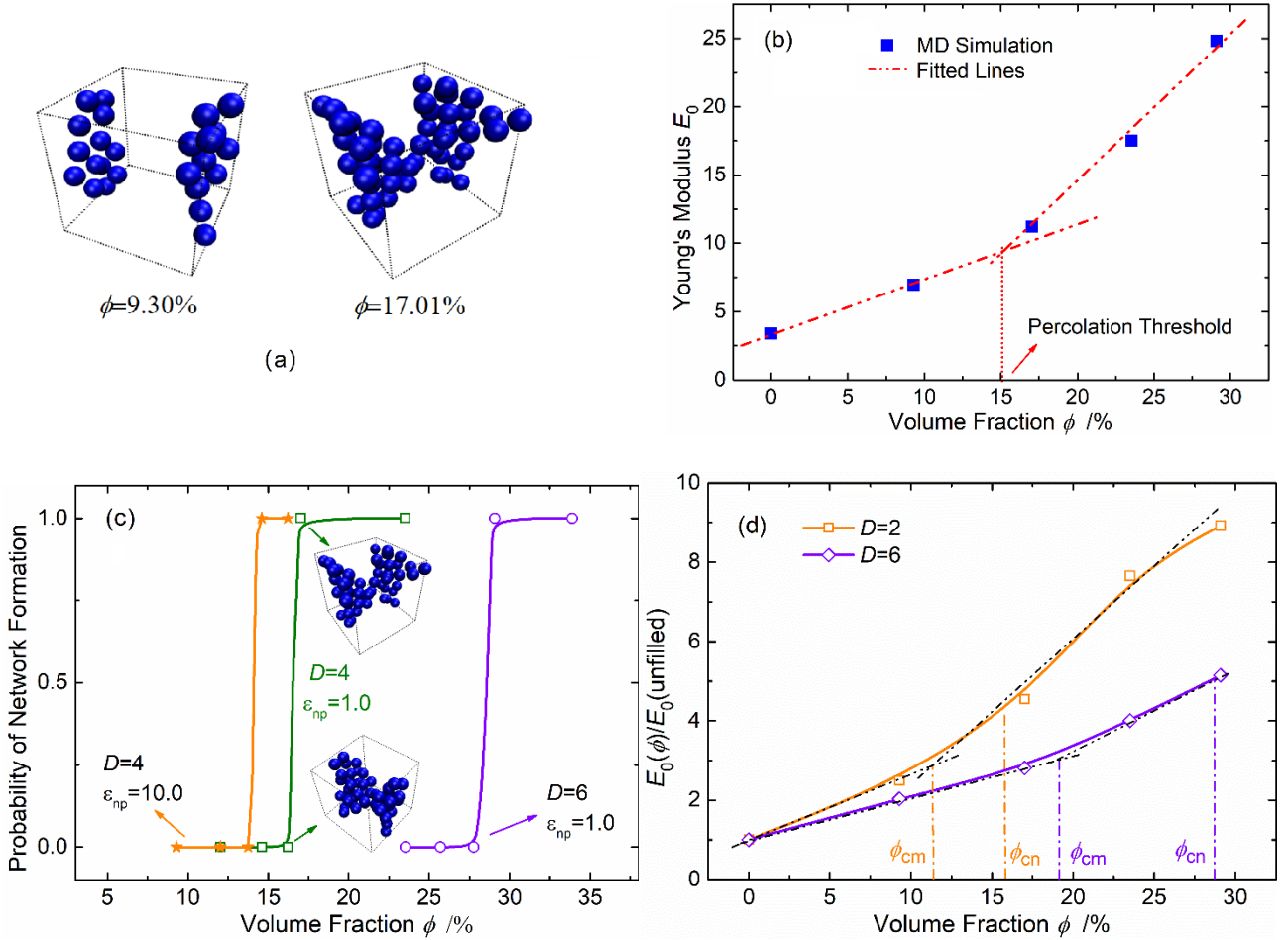


Fig. S2. (a) Snapshot of equilibrated simulation systems at the volume fraction of 9.30% and 17.01%. (b) Young's modulus as a function of volume fraction. The nanoparticle diameter is $D=4$, and the particle-polymer interaction strength is $\epsilon_{np}=1.0$. (c) Probability of network formation as a function of nanoparticle volume fraction for different simulated systems. (d) Comparison of the percolation threshold ϕ_{cm} from the mechanical reinforcement method and that from nanoparticle cluster percolation analysis ϕ_{cn}

To quantitatively identify the percolation threshold, we have evaluated the probability of three-dimensional network formation as a function of nanoparticle volume fraction. At the particle-polymer interaction of $\epsilon_{np}=1.0$, two neighboring nanoparticles of diameter $D=4$ are considered to form a cluster if their center-to-center distance is smaller than 4.25σ , according to the radial distribution functions between nanoparticles $g_{nn}(r)$ in Fig. 2b. That is to say, two nanoparticles with their gap less than 0.25σ are directly connected; such a judgement condition is also applied in the cases of $D=2$ and $D=6$ at $\epsilon_{np}=1.0$. However, when the particle-polymer interaction is too strong (e.g., $\epsilon_{np}=5.0$ and 10.0) to form nanoparticle-polymer-nanoparticle sandwich structures (Fig. 2b), a critical gap distance of 1.25σ is used to determine the formation of nanoparticle clusters bridged by polymer layer. A three-dimensional nanoparticle network forms once the largest nanoparticle cluster spans the whole simulation box in three-dimensional directions. Such a criterion is somewhat arbitrary but at a very reasonable level [4]. From Fig. R3 below, it can be seen that the percolation threshold ϕ_{cn} of nanoparticles with diameter of $D=4$ is approximately 16.5%, while the ϕ_{cn} for diameter $D=6$ is much larger, close to 28.0%. Besides, at high particle-polymer interaction of $\epsilon_{np}=10.0$, a three-dimensional nanoparticle network bridged by polymer layers is expected to form beyond the volume fraction of $\sim 13.5\%$.

In the context of $D=4$ and $\epsilon_{np}=1.0$, the percolation threshold ($\phi_{cm}\sim 15\%$) from the mechanical reinforcement method and that from nanoparticle cluster percolation analysis ($\phi_{cn}\sim 16.5\%$) are quite close. However, we think this may just be a coincidence. Firstly, the percolation transition for nanoparticle clusters is a first-order phase transition, which expects an abrupt transition of physical quantities. The mechanical reinforcement of PNCs, however, behaviors more like a second-order phase transition [5-6]. Such a discrepancy reflects that the critical mechanical phenomenon for PNCs is not a pure percolation transition, for which the mechanical reinforcement is much more complicated, especially with polymer chains serving a fairly important role. For example, the bound polymer layers around nanoparticles also contribute largely to the mechanical reinforcement, and when the bound polymer layers percolates (undoubtedly below the percolation threshold of nanoparticle network, ϕ_{cn}), the mechanical properties will be significantly enhanced, with higher Young's modulus than expected below ϕ_{cn} , resulting in a less steep percolation transition at the nanoparticle network formation point. Besides, during the formation of nanoparticle aggregates

before the eventual establishment of long-ranged network, some polymer chains are likely to be trapped in the local clusters [7], which will also make the percolation transition of filler network more moderate. In general, owing to the important contribution of polymer chains to the mechanical properties, the percolation transition for mechanical reinforcement is not entirely/decisively (maybe on a very large scale) dependent on the nanoparticle network formation, and thus behaviors more like a second-order phase transition.

Secondly, by comparing the percolation threshold ϕ_{cm} from the mechanical reinforcement method and that from nanoparticle cluster percolation analysis ϕ_{cn} in other simulation systems, as shown in Fig. R2 above, it can be found that the two percolation thresholds are not identical. Specifically, the percolation threshold ϕ_{cm} from the mechanical reinforcement method is always smaller than that from nanoparticle cluster percolation analysis ϕ_{cn} . Such a discrepancy confirms the above-discussed point that the percolation transition of mechanical reinforcement does not fully depend on the nanoparticle network formation.

In conclusion, the critical mechanical phenomenon for PNCs is not a pure percolation transition of nanoparticle clusters, and if we discuss such a behavior of mechanical reinforcement in the framework of percolation theory, then the mechanical reinforcement method can give a good indication of the percolation threshold. From Figure 5a, below a critical nanoparticle loading, the increase of Young's modulus with filler volume fraction is approximate to linearity in a consistent manner with hydrodynamic effect. Beyond the critical filler loading, the Young's modulus increases exceptionally with the filler content, owing to the strong filler-filler interaction including the short-ranged inter-aggregate association via direct contacting or long-ranged filler network bridged by bound polymer layers. Notably, the global filler network developed by high particle concentration makes more significant contribution to the mechanical reinforcement than merely the disconnected bound polymer layers around fillers. In fact, this percolation threshold ϕ_{cm} from MD simulation (~15%) is close to the experimental observation (~11%) for the silica-filled poly(vinyl acetate) systems [1] and that for PS/silica-filled polybutylacrylate systems (~15.8%) [8].

References

- (1) Bogoslovov, R.B., Roland, C.M., Ellis, A.R., Randall, A.M. and Robertson, C.G., Effect of silica nanoparticles on the local segmental dynamics in poly (vinyl acetate). *Macromolecules*, 2008, 41(4), pp.1289-1296.

- (2) Wang, Z., Liu, J., Wu, S., Wang, W. and Zhang, L., Novel percolation phenomena and mechanism of strengthening elastomers by nanofillers. *physical chemistry chemical physics*, 2010, 12(12), pp.3014-3030.
- (3) Chung, K.T., Sabo, A. and Pica, A.P., Electrical permittivity and conductivity of carbon black - polyvinyl chloride composites. *Journal of Applied Physics*, 1982, 53(10), pp.6867-6879.
- (4) Feng, Y., Zou, H., Tian, M., Zhang, L. and Mi, J., Relationship between dispersion and conductivity of polymer nanocomposites: a molecular dynamics study. *The Journal of Physical Chemistry B*, 2012, 116(43), pp.13081-13088.
- (5) Jin, Y., Huang, G., Han, D., Song, P., Tang, W., Bao, J., Li, R. and Liu, Y., Functionalizing graphene decorated with phosphorus-nitrogen containing dendrimer for high-performance polymer nanocomposites. *Composites Part A: Applied Science and Manufacturing*, 2016, 86, pp.9-18.
- (6) Chen, J., Cui, X., Sui, K., Zhu, Y. and Jiang, W., Balance the electrical properties and mechanical properties of carbon black filled immiscible polymer blends with a double percolation structure. *Composites Science and Technology*, 2017, 140, pp.99-105.
- (7) Gauthier, C., Reynaud, E., Vassoille, R. and Ladouce-Stelandre, L., Analysis of the non-linear viscoelastic behaviour of silica filled styrene butadiene rubber. *Polymer*, 2004, 45(8), pp.2761-2771.
- (8) Chabert, E., Bornert, M., Bourgeat-Lami, E., Cavaillé, J.Y., Dendievel, R., Gauthier, C., Putaux, J.L. and Zaoui, A., Filler-filler interactions and viscoelastic behavior of polymer nanocomposites. *Materials Science and Engineering: A*, 2004, 381(1-2), pp.320-330.

Part II. Comparison of Simulation Results with Experimental Data

(1) Comparison of the Payne effect of Polymer Nanocomposites

The strain-induced nonlinear behavior of elastic modulus in our simulation is found to be quite similar to the experimentally observed “Payne effect”, whose feature is actually embodied in the dependence of dynamic storage modulus on shear amplitude. In order to quantitatively compare the results from our simulation and real experiments on a reasonable level, we aim to evaluate them in terms of the Payne effect magnitude and the characteristic strain. The Payne effect magnitude is given by

$$\Delta E/E_0 = (E_0 - E_\infty)/E_0$$

where E_0 and E_∞ are the elastic modulus at the initial plateau and at the plateau of large deformation, respectively (for experimental results, the storage modulus versus shear amplitude). The characteristic strain of the decay for the elastic modulus, ε_c , which is defined as the strain (shear amplitude) when the elastic modulus decays to a certain value (e.g., $E_c/E_0 = 1/2$). The characteristic strain measures the decay rate of elastic modulus with strain and can also serve to quantify the nonlinear behavior of PNCs.

Table S1 displays the data extracted from both the current research and some literatures relating to experimental research on PNCs. We note that the experimental results of $\Delta E/E_0$ and ε_c in Table S1 are estimated on the basis of the figures in those literatures, and thus the statistical errors would be as large as 10%-20%. From Table S1, we find that the $\Delta E/E_0$ and the ε_c that are obtained from our MD simulations can be matched to some extent to some certain specific experimental systems. Specifically, our simulation systems filled with spherical particles behave in a manner similar to that of realistic silica-filled rubber nanocomposites (ref. 2 & ref. 3) in terms of the Payne effect.

Table S1. Comparison of the Payne effect extracted from the current MD simulation study and the literatures relating to experiment research

System	φ^a	D^b	ε_{np}^c	$\Delta E/E_0^d$	ε_c^e	Ref.
Current Simulation ^f	9-29 vol%	2σ - 6σ	0.1-10.0	0.84-0.96	0.03-0.05	--
SBR/Silica	5-30 wt%	13 nm	Surface treated	0.17-0.43	0.09-0.2	[1]
PBD/Silica	2-29 vol%	15 ± 5 nm	Surface treated	0.8-0.98	0.02-0.1	[2]
SR/Silica	N/A	N/A	Untreated	0.91-0.92	0.007-0.01	[3]

SSBR/Silica	20-40 phr	12 nm	Surface treated	0.63-0.78	0.1-0.3	[4]
PAM/Silica	5-15 vol%	15 nm	Surface treated	0.1-0.4	N/A	[5]
NR/CB ^g	7-18 vol%	29 nm, 50 nm	Untreated	0.20-0.64	0.1-0.8	[6]
NR/CB	28 vol%	N/A	Untreated	0.61	0.05	[3]
SSBR/CB	20-40 phr	25 nm	Untreated	0.63	0.18-0.3	[4]
CBG ^h	N/A	N/A	Untreated	0.97	0.002	[7]

^a Filler volume fraction (weight fraction), ^b Filler Diameter, ^c Polymer-filler interaction strength, ^d Elastic modulus (storage modulus) drop with strain (relative to the original modulus), ^e Characteristic strain (shear amplitude) of the decay for the elastic modulus, ^f PNCs filled with spherical particles, ^g Carbon Black, ^h Carbon black gel extracted from NR compounds filled with 40-70 phr carbon black

Table S2. Polymer Abbreviations

Abbreviation	Polymer
SBR	styrene-butadiene rubber
PBD	1,4-polybutadiene
SR	silicone rubber (poly-dimethyl-diphenyl-siloxane)
SSBR	solution-polymerized styrene butadiene rubber
PAM	poly-(acrylamide)
PVAc	poly-(vinyl acetate)
EPDM	ethylene propylene diene monomer rubber
CPI	cis-polyisoprene
TPI	trans-polyisoprene
NBR	nitrile butadiene rubber
PSETS	poly(Sty-b-[EVBI _m][Tf ₂ N]-b-Sty) triblock copolymer
PIB	polyisobutylene

References

- (1) Gauthier, C., Reynaud, E., Vassoille, R. and Ladouce-Stelandre, L., Analysis of the non-linear viscoelastic behaviour of silica filled styrene butadiene rubber. *Polymer*, 2004, 45(8), pp.2761-2771.
- (2) Zhu, Z., Thompson, T., Wang, S.Q., von Meerwall, E.D. and Halasa, A., Investigating linear and nonlinear viscoelastic behavior using model silica-particle-filled polybutadiene. *Macromolecules*, 2005, 38(21), pp.8816-8824.
- (3) Chazeau, L., Brown, J.D., Yanyo, L.C. and Sternstein, S.S., Modulus recovery kinetics and other insights into the Payne effect for filled elastomers. *Polymer composites*, 2000, 21(2), pp.202-222.
- (4) Stockelhuber, K.W., Svistkov, A.S., Pelevin, A.G. and Heinrich, G., Impact of filler surface modification on large scale mechanics of styrene butadiene/silica rubber composites. *Macromolecules*, 2011, 44(11), pp.4366-4381.
- (5) Yang, J. and Han, C.R., Dynamics of silica-nanoparticle-filled hybrid hydrogels: nonlinear viscoelastic behavior and chain entanglement network. *The Journal of Physical Chemistry C*, 2013, 117(39), pp.20236-20243.

- (6) Omnès, B., Thuillier, S., Pilvin, P., Grohens, Y. and Gillet, S., Effective properties of carbon black filled natural rubber: Experiments and modeling. *Composites Part A: Applied Science and Manufacturing*, 2008, 39(7), pp.1141-1149.
- (7) Gan, S., Wu, Z.L., Xu, H., Song, Y. and Zheng, Q., Viscoelastic behaviors of carbon black gel extracted from highly filled natural rubber compounds: insights into the Payne effect. *Macromolecules*, 2016, 49(4), pp.1454-1463.

(2) Comparison of the Mechanical Reinforcement of Polymer Nanocomposites

Fig. S3 shows a quantitative comparison between the mechanical reinforcement magnitude of the current research and that of some literatures relating to experimental research on PNCs. The mechanical reinforcement magnitude is defined as the Young's modulus of PNCs normalized with that of unfilled polymer, $E_0(\phi)/E_0(\text{unfilled})$. It should be noted that the experimental results in Fig. S3 are estimated on the basis of the figures in those literatures, and thus the statistical errors would be as large as 10%-20%. From Fig. S3, it is seen that the mechanical reinforcement magnitude $E_0(\phi)/E_0(\text{unfilled})$ from our MD simulations is within the range of common experimental systems, depending on the particle type and size, and the particle-polymer interaction. Especially, the mechanical reinforcement for the simulation system of $D=4$ and $\epsilon_{np}=1.0$ is in good agreement with that of carbon black-filled nature rubber composite system in ref. 2.

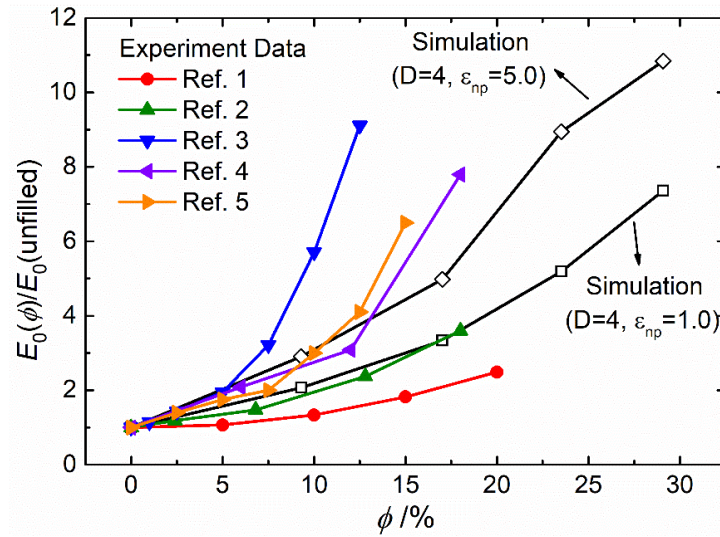


Fig. S3. Mechanical reinforcement extent, in terms of Young's modulus of nanoparticle-filled systems normalized by that of unfilled system, as a function of filler volume fraction. References are listed below. Details of filler parameters are shown in Table S3.

Table S3. Some Filler Parameters in the literatures relating to experiment research

System	D^a	ϵ_{np}^b	Ref.
Current Simulation ^c	4σ	1.0, 5.0	--
PAM/Silica	15 nm	Surface treated	[1]
NR/CB ^d	29 nm	Untreated	[2]
PVAc/Silica	~ 7 nm	Untreated	[3]
EPDM/CB	N/A	Surface treated	[4]
PBD/Silica	N/A	Surface treated	[5]

^a Filler Diameter, ^b Polymer-filler interaction strength, ^c PNCs filled with spherical particles, ^d Carbon Black

References

- (1) Yang, J. and Han, C.R., Dynamics of silica-nanoparticle-filled hybrid hydrogels: nonlinear viscoelastic behavior and chain entanglement network. *The Journal of Physical Chemistry C*, 2013, 117(39), pp.20236-20243.
- (2) Omnès, B., Thuillier, S., Pilvin, P., Grohens, Y. and Gillet, S., Effective properties of carbon black filled natural rubber: Experiments and modeling. *Composites Part A: Applied Science and Manufacturing*, 2008, 39(7), pp.1141-1149.
- (3) Sternstein, S.S. and Zhu, A.J., Reinforcement mechanism of nanofilled polymer melts as elucidated by nonlinear viscoelastic behavior. *Macromolecules*, 2002, 35(19), pp.7262-7273.
- (4) Mokhothu, T.H., Luyt, A.S. and Messori, M., Reinforcement of EPDM rubber with in situ generated silica particles in the presence of a coupling agent via a sol-gel route. *Polymer Testing*, 2014, 33, pp.97-106.
- (5) Wong, W.K., Ourieva, G., Tse, M.F. and Wang, H.C., April. Filler-filler interaction and filler-polymer interaction in carbon black and silica filled Exxpro™ polymer. In *Macromolecular Symposia*, 2003, (Vol. 194, No. 1, pp. 175-184). Weinheim: WILEY-VCH Verlag.

(III) Comparison of Activation Energy of Polymer Nanocomposites

According to the research work of Liu et al. (Macromolecules 2006, 39, 8867), the polymers will show an Arrhenius-like temperature dependence at the temperature larger than $1.3T_g$ (T_g is the glass transition temperature), and based on the Gibbs-DiMarzio lattice model (J. Polym. Sci. 1959, 40, 121), the characteristic temperature T_0 in VFT equation is expected to show the Adams-Gibbs relation:

$$T_0 = 0.77T_g$$

In our simulation, the glass transition temperature is approximately $T_g = 0.46$, and the characteristic temperature is estimated to be $T_0 = 0.39$, which is close to the value of $0.77T_g$ (~ 0.354), roughly in consistent with the Adams-Gibbs relation.

Besides, Table S4 shows the data of activation energy extracted from both the current research and some literature relating to experiment. It is found the activation energy of our simulation model are almost 1-2 order of magnitude lower than that of experiment. Such a decrease in the temperature dependence of polymer dynamics is originated from coarse-graining the dynamics of a model polymeric material and (J.F. Douglas et al., Macromolecules, 2017, 50, 8787). Despite the deviations of the coarse-grain model from real experiments in activation energies, the main conclusions obtained in this research will not change.

Table S4. Activation energy derived from experiment research

System	ε^a (kcal/mol)	E^b (kcal/mol)	E/ε	Ref.
Current Simulation ^c	$1.0 \varepsilon/k_B T$	$0.12 \varepsilon/k_B T$	0.12	--
PS	0.96	8.31	8.65	[1]
PIB	~ 0.89	10-24	11.2-26.9	[2]
CPI/NBR	~ 0.61	3-8	5.0-13.3	[3]
PSETS	~ 0.96	2.78	2.89	[4]
CPI/TPI	~ 0.61	2.4-13.1	3.9-21.5	[5]

^a Monomer-monomer interaction strength from Ref. Kremer, K.; Grest, G. S., J. Chem. Phys. 1990, 92, 5057; ^b Activation energy from VFT theory; ^c PNCs filled with spherical particles ($D=4$, $\phi=17.01\%$)

References

(1) Fakhrāai, Z. and Forrest, J.A., Probing slow dynamics in supported thin polymer films. Physical review letters, 2005, 95(2), p.025701.

- (2) Hopkins, I.L., The Ferry reduction and the activation energy for viscous flow. *Journal of Applied Physics*, 1953, 24(10), pp.1300-1304.
- (3) Baboo, M., Gupta, S., Sharma, K. and Saxena, N.S., Dynamic mechanical, mechanical and thermal analysis of CPI/NBR blends: effect of blend composition and crosslink density. *Polymer Bulletin*, 2016, 73(7), pp.2003-2018.
- (4) Green, M.D., Wang, D., Hemp, S.T., Choi, J.H., Winey, K.I., Heflin, J.R. and Long, T.E., Synthesis of imidazolium ABA triblock copolymers for electromechanical transducers. *Polymer*, 2012, 53(17), pp.3677-3686.
- (5) Baboo, M., Sharma, K. and Saxena, N.S., Viscosity, glass transition and activation energy of solid cis-polyisoprene and trans-polyisoprene blends. *Phase Transitions*, 2011, 84(11-12), pp.901-907.

The bond orientation is measured by the second-order Legendre polynomials $\langle P_2 \rangle$:

$$\langle P_2 \rangle = \frac{3\langle \cos^2 \theta \rangle - 1}{2}$$

where θ denotes the angle between a given element (two adjoining monomers in a polymer chain) and the reference direction (the stretching direction). The possible values of $\langle P_2 \rangle$ range from -0.5 to 1.0. Specifically, $\langle P_2 \rangle = -0.5$ indicates a perfect orientation perpendicular to the reference direction, $\langle P_2 \rangle = 0.0$ represents a random orientation of the segments and $\langle P_2 \rangle = 1.0$ means a perfect alignment parallel to the reference direction.

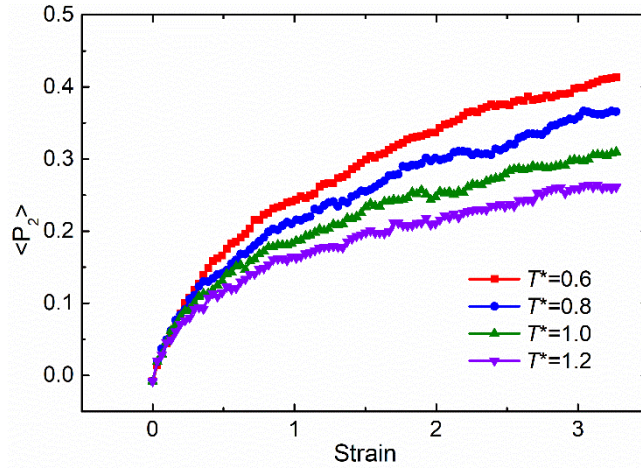


Fig. S4. The bond orientation $\langle P_2 \rangle$ as a function of strain at different system temperatures. ($D=4$, $\phi=17.01\%$, $\varepsilon_{np}=1.0$ and $\varepsilon_{nn}=1.0$)

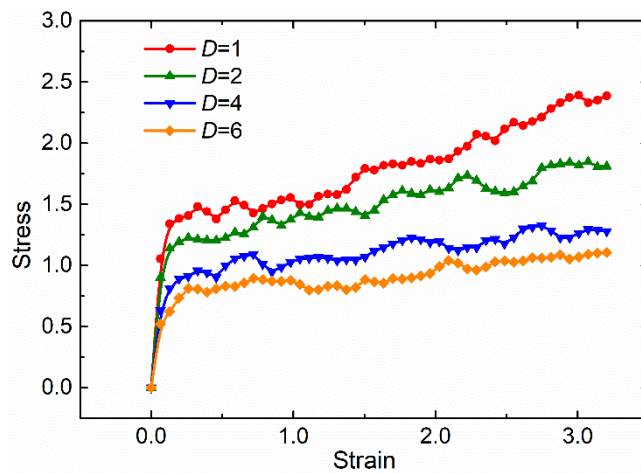


Fig. S5. Stress-strain curves with different nanoparticle diameters at a volume fraction of $\phi=17.01\%$.